Physica A 394 (2014) 145–157

Contents lists available at ScienceDirect

Physica A

journal homepage: www.elsevier.com/locate/physa

Spatial social dilemmas: Dilution, mobility and grouping effects with imitation dynamics

Mendeli H. Vainstein *, Jeferson J. Arenzon

Instituto de Física, Universidade Federal do Rio Grande do Sul, CP 15051, 91501-970 Porto Alegre RS, Brazil

HIGHLIGHTS

- We systematically explore the parameter space of social dilemmas in a 2d lattice.
- We elaborate detailed phase diagrams with and without dilution and mobility.
- We explain the microscopic mechanisms responsible the increase of cooperation.

ARTICLE INFO

Article history:
Received 17 September 2013
Available online 25 September 2013

Keywords:
Game theory
Prisoner's dilemma
Snowdrift
Cooperation
Mobility

ABSTRACT

We present an extensive, systematic study of the Prisoner's Dilemma and Snowdrift games on a square lattice under a synchronous, noiseless imitation dynamics. We show that for both the occupancy of the network and the (random) mobility of the agents there are intermediate values that may increase the amount of cooperators in the system and new phases appear. We analytically determine the transition lines between these phases and compare with the mean field prediction and the observed behavior on a square lattice. We point out which are the more relevant microscopic processes that entitle cooperators to invade a population of defectors in the presence of mobility and discuss the universality of these results.

1. Introduction

Spatially distributed viscous populations sustain cooperation due to the fact that individuals form clusters for self-defense and mutual support (see Refs. [1–5] and references therein for reviews). Nonetheless, the conditions for the appearance and the properties of such cooperative regions are not fully understood both in real and model systems. Given that the spatial localization allows a continuing interaction within the local neighborhood, the population viscosity may prevent defectors from invading the whole population, what otherwise occurs under random mixing. Once the high viscosity constraint is relaxed and density permits [6,7], agents are able to diffuse. There are many ways in which mobility [8–12] can be implemented: it may be random [13–20], strategy dependent [21], driven by payoff [22–25], success [26–28] or neighborhood [29–34], take or not [25,33,35] excluded volume into account, be local or long ranged, occur on a discrete lattice (regular or complex) [13–18,22,28,30,36], in continuous space [25,33,35] or in a fully connected system, it may be explicit or included as a cost [36], etc. Our previous results [13,17] show that even in the simplest framework of random, non-contingent mobility of unconditional agents, diffusion is remarkably able to enhance cooperation within broad conditions. Besides the typical interval between generations, a new timescale is involved when mobility is taken into account in this simple model, the diffusion characteristic time. If the typical time a step takes to occur is much larger than the generation interval, the high viscosity limit may be a reasonable approximation. On the other hand, if diffusion is fast, the behavior should

* Corresponding author. Tel.: +55 5133086474.
E-mail address: mendeli.vainstein@ufrgs.br (M.H. Vainstein).

0378-4371/$ – see front matter
http://dx.doi.org/10.1016/j.physa.2013.09.032

approach, density permitting, the fully mixed case. An interesting regime is when both timescales are similar: in that case the order in which the dynamics is performed, whether the offspring generation occurs before of after the diffusion step, has important consequences for the cooperative outcome [13,17] and is often neglected.

We consider a 2×2 game with pure, unconditional strategies: cooperation (C) or defection (D). Cooperation involves a benefit to the recipient at the expense of the provider. Depending on the mutual choice, the earned payoff is: a reward R (punishment P) if both cooperate (defect), S (sucker's payoff) and T (temptation) if one cooperates and the other defects, respectively. In the Prisoner's Dilemma (PD) game, the above payoffs are ranked as $T > R > P > S$ and $2R > T + S$. Thus, it clearly pays more to defect whatever the opponent's strategy: the gain will be $T > R$ if the other cooperates and $P > S$ in the case of defection. The dilemma appears since if both play D they get P, what is worse than the reward R they would have obtained had they both played C. On the other hand, there are situations when mutual defection is even worst than being exploited, and $P < S$. This defines a different game, in which $T > R > S > P$, known as Chicken or Snowdrift (SD) [37]. Without loss of generality, we renormalize all values such that $R = 1$ and $P = 0$, the values of T and S remaining as the parameters that define the nature of the game.

In a randomly mating population (mean field limit) with both C and D strategies present, defection will be the most rewarding strategy for the PD game, independently of the opponent's choice. As shown by Nowak and May [38], when spatial correlations are included in the population, for example by placing the agents on a lattice, cooperators form clusters in which the benefits of mutual cooperation can outweigh losses against defectors, thus enabling cooperation to be sustained, in contrast to the spatially unstructured game, where defection is favored (these effects of the spatial structure may be due to either the distribution of agents in space or to the context preservation during the dynamics, see Ref. [39] for a detailed account). Since then, the original Nowak–May version was extended and modified in several different ways (see Ref. [3] and references therein). Once placed on a network, by analyzing the possible neighborhoods [40,41], one can divide the parameter space into several regions with different levels of cooperation and spatial structures. In this work we extend their analysis to include the SD game, dilution and mobility of the agents, locating all transitions between distinct phases. In the presence of defects (density $\rho < 1$) but without mobility, all transitions already present in the full system remain, but a few others appear because of the larger number of possible local configurations. Remarkably, when diffusive processes are also present, in which an agent jumps to an empty site with probability m, whether new phases appear or not depends on the chosen dynamics.

A systematic study of how often spatial structure favors cooperative behavior has been the program of a few papers (see, for example, Refs. [39,41–45]). The task is not simple due to the multitude of different dynamical rules and lattice geometries that may be considered [3]. Nonetheless, we complement these previous works by including dilution and mobility while considering a parallel imitation rule, in which each individual combats with all its closest neighbors (if any), accumulates the corresponding payoff and then may either move or try to generate its offspring. In the reproduction step, each player compares its total payoff with those of its neighbors and changes strategy, following the one with the greatest payoff among them. This strategy changing updating rule preserves the total number of individuals, thus keeping ρ constant. Notice that although there is no noise in this updating rule, the random mobility to be considered here now has a similar role and prevents the system from becoming stuck on shallow minima. Initially, an equal number of cooperators and defectors are randomly placed on a two dimensional square lattice of linear size L and periodic boundary conditions, and the system is allowed to evolve until a stationary state is attained, when the measures are thus taken.

The paper is organized as follows. In the next section, the phase diagrams for fully occupied and diluted (with and without random mobility) are obtained and compared with numerical simulations and the mean field prediction. We then discuss the possible mechanisms leading to the enhancement or inhibition of cooperation and finally present our conclusions.

2. Phase diagrams

When spatial correlations are not relevant, as when all agents interact with all others (mean field limit), the phase diagram is easily obtained, Fig. 1 (see, e.g., Ref. [42]). For $P = 0$ and $R = 1$ there are two transition lines, one at $T = 1$ and other at $S = 0$, dividing the TS plane into two sections above $T = 1$,[1] the PD game for $S < 0$ and the SD for $S > 0$. When $S < 0$ (and $T > 1$), defectors dominate and the relative[2] density of cooperators, ρ_c, is equal to 0. On the other hand, for $S > 0$ (and again $T > 1$), cooperators and defectors coexist with $\rho_c = S/(S + T - 1)$.

When spatial localization becomes an important factor, the corresponding phase diagram can be constructed by analyzing all the neighborhood configurations that are possible in the confrontation between two agents having different strategies. The transitions present in the phase diagram consider all such configurations, irrespective of their probability of occurrence. If a given local configuration is rather rare, it might happen that our finite time simulations on a finite lattice are not able to sample it and, as a consequence, two phases might look rather similar or perhaps identical. In the following, we consider a square lattice with the von Neumann neighborhood (nearest neighbors only) and without self-interaction, but the results can be extended to other lattices and neighborhoods, although the complexity of the task may vary. Unless

[1] There are indeed two more regions for $T < 1$, but they are not considered here: for $S > 0$ (Harmony game), $\rho_c = 1$, and for $S < 0$ (Stag Hunt game), the amount of cooperators depends on their initial density: if it is larger (smaller) than $S/(S + T - 1)$, then $\rho_c = 0$ (1).

[2] In this paper, all densities are relative to the total number of agents, not sites.

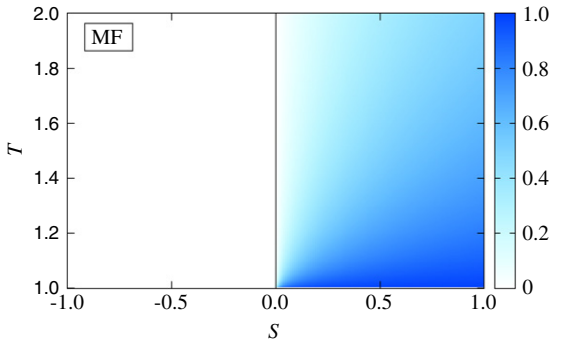

Fig. 1. Mean field (fully mixed) phase diagram for $P = 0$ and $T > R = 1$. The solid line shows the transition from the defector dominated phase ($S < 0$, PD game) to the coexistence one ($S > 0$, SD game). The scale at the right indicates the density of cooperators, $\rho_c = S/(S + T - 1)$, for $S > 0$, with darker colors assigned to larger ρ_c.

specified, all simulated systems have a linear length of $L = 100$, and results are averaged over 100 different initial random configurations such that $\rho_c(0) = \rho_d(0) = \rho/2$. The number of initial steps neglected before the asymptotic state depends on the density and mobility. In order to compare with our previous works, we consider the "imitate-the-best" dynamics, in which all individual's strategies are synchronously replaced by the strategy adopted by the individual with the highest collected payoff in the neighborhood. Besides this synchronous updating of the strategies, a Monte Carlo Step (MCS) also comprises an attempt, by each agent, to diffuse: each agent blindly chooses a neighboring site and, if it is empty, jumps to it with probability m. Using the notation of Schweitzer et al. [41], K_θ^n denotes the local occupation pattern and $p(K_\theta^n)$ the payoff acquired by an individual in such a configuration. Here, $n \in \{0, 1, 2, 3, 4\}$ gives the total number of cooperators in the local neighborhood and $\theta \in \{0, 1\}$ describes whether the center cell is occupied by a defector or a cooperator, respectively. In the absence of empty sites, the number of defectors in a neighborhood is $4 - n$. The construction of the phase diagram amounts to the analysis of all the possible confrontations of $K_0^{n_0}$ and $K_1^{n_1}$, for $n_0 \in \{1, 2, 3\}$ and $n_1 \in \{0, 1, 2, 3, 4\}$. The value of $n_0 = 0$ is not important because a D having four D neighbors will either be surrounded by Ds with the same payoff or with higher payoff D players that have C neighbors, since $T > P$. The value of $n_0 = 4$ is not considered because with the chosen payoffs ($T > R$), a D with four C neighbors always has the highest possible payoff. This value might play a role when considering games in which ($T < R$), as in the Stag Hunt [42,46].

2.1. Full occupancy ($\rho = 1$)

We initially consider the simpler case without empty sites ($\rho = 1$), in which obviously no mobility, as implemented here, is possible. For the PD and SD games, the following family of functions compare the payoffs that result from all possible confrontations of a D and a C, having local neighborhoods given by $K_0^{n_0}$ and $K_1^{n_1}$, respectively,

$$f_{n_0 n_1} = \frac{n_1 R + (4 - n_1)S - (4 - n_0)P}{n_0}. \tag{1}$$

If $T > f_{n_0 n_1}$, then the D with local configuration $K_0^{n_0}$ will beat the C with local configuration $K_1^{n_1}$; if $T < f_{n_0 n_1}$, then the D will beaten; and if $T = f_{n_0 n_1}$, there will be a draw between the two players. Indeed, the behavior at a transition point may be different from the neighboring regions, what makes each segment between line crossings a phase in itself. The phase diagram will then be composed of the regions defined by all these functions, together with the inequalities that define the games. For given values of R, P and n_i in the allowed ranges, these 15 functions, which can be separated into 3 groups depending on n_0, represent the values of T where there are transitions which divide the parameter space into different phases. Without loss of generality, we can take $R = 1$, so that the above functions will describe planes in the three dimensional space of T, P and S, leading to a complex phase diagram in three dimensions. The usual choice of $P = 0$ takes a 2d cross-section of this three dimensional parameter space allowing a simpler description of the phase diagram, as shown in Fig. 2. Within each phase, the behavior is the same, and it is enough to numerically study a single representative point for synchronous imitation dynamics, as can be seen in Fig. 3, where different simulation points in the same phase lead to the same outcome. The transition between two neighboring phases is usually discontinuous, the density of cooperators presenting abrupt jumps when a transition line is crossed, as can be seen in Fig. 3. The dashed lines in Fig. 2 are not transition lines, but two common parametrizations of the payoff matrix for these games. The diagonal dashed line considers $T = 1 + r$ and $S = 1 - r$ (such that $T + S = 2$), where r is a parameter. The second parametrization line, the vertical one at $S = 0$, is exactly at the border between the SD and PD games, and is known as the weak PD. Notice that several phases are left out with such parametrizations.

Fig. 3 (top) shows, for $T = 1.4$, the fraction of cooperators as a function of S, along with the mean field result. Two important features can be noticed. First of all, while for $S < 0$ the spatial correlations significantly increase the amount of

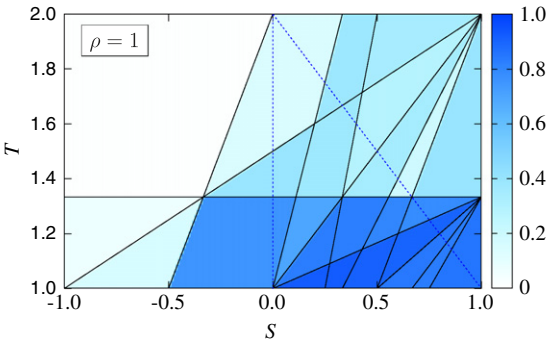

Fig. 2. Two dimensional cross section of the phase diagram displaying the asymptotic density of cooperators, for full occupancy ($\rho = 1$) and $P = 0$, $T > R = 1$ and $S < R$. The solid lines represent the functions $f_{n_0 n_1}$ which delimit different phases (functions having the same n_0 intercept at the same point on the line $S = 1$). White regions are dominated by defectors, while the blue/gray ones have some fraction of cooperators, its density indicated by the scale on the right. The color code does not represent what happens at the transition lines, where draws happen and the fraction of cooperators may differ from the two neighboring phases. Notice that, for a fixed T, ρ_c is not monotonic in S (see Fig. 3). The dotted line $T = 2 - S$ is a usual choice for the payoff matrix: $T = 1 + r$ and $S = 1 - r$, r being a payoff parameter. Another traditional choice, also shown as a dotted line, is $S = 0$ and separates the PD and SD games (however, this is a transition line in the mean field case). The horizontal line at $T = 4/3$ separates the low C region (above) from the high C one (below). (For interpretation of the references to color in this figure legend, the reader is referred to the web version of this article.)

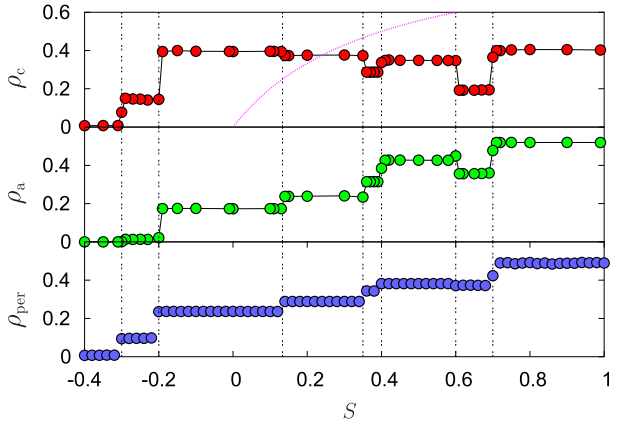

Fig. 3. (Top) Asymptotic density of cooperators as a function of S for $T = 1.4$, when the lattice is fully occupied ($\rho = 1$) and the initial state is random. Notice both the abrupt change of ρ_c when a transition line is crossed and the non monotonic behavior of ρ_c. On those lines, the value of ρ_c may be very different from the neighboring phases. Also shown is the fully-mixed result, for which the density of cooperators is non zero only for $S > 0$ and is an increasing function of S in that interval. Notice that for the region around the weak PD ($S = 0$), spatial correlations enhance cooperation [38]. (Middle) Fraction of active sites ρ_a for the same parameters. Besides the transition points, only the $0.6 < \rho < 0.7$ region breaks the increasing monotonicity. (Bottom) The fraction ρ_{per} of cooperator–defector pairs (to be compared with the snapshots of Fig. 4).

cooperation when compared to the mean field limit, this is not always the case for $S > 0$ (SD). Indeed, for $S \gtrsim 0.24$, the mean field curve lies above the lattice results, while for $0 < S \lesssim 0.24$, spatial correlation improves cooperation. The second evident feature is the non-monotonicity of ρ_c: as S increases, one would intuitively expect larger levels of cooperation; instead, some regions (most prominently, around $S = 0.65$) present a smaller than expected fraction of cooperators. A large amount of cooperation is related to the existence of a long tail in the distribution of group sizes (a group is defined as a set of neighboring, same strategy agents), as is the case, for example, for $S = 0$ and 0.8. On the other hand, for $S = 0.65$ the system has a much lower level of cooperation and very few large clusters. This can be checked in Fig. 4 in which some characteristic snapshots are shown for $T = 1.4$ and 1.8. For $S = 0$, leftmost snapshot, the minimal cooperative cluster able to grow is 2×2, while smaller or linear clusters are removed in the first steps of the dynamics. The surviving clusters are far away from each other and grow through flat edges (with at least two cooperators) while diagonals are stable (although both cooperators and defectors at a diagonal interface have two neighboring cooperators, and $p(K_1^2) < p(K_0^2)$, the cooperators are backed up by interior cooperators with higher payoffs). Thus, rather large and compact clusters may grow before starting to interfere with each other. Once they get close enough, defectors trapped between these clusters will have cooperators at both sides, and therefore will acquire a large payoff and reproduce. These defector clusters will grow as well until a dynamical equilibrium is achieved. For $S = 0.5$, second snapshot, since $p(K_1^0) > p(K_0^1)$, single cooperators are able to seed a growing cluster and survive in a sea of defectors. The clusters are much less compact than in the previous case and the lattice is populated by those smaller clusters that were decimated in the $S = 0$ case. Being less compact, clusters increase the amount of interactions between cooperators and defectors and both the fraction of interface and active sites increase.

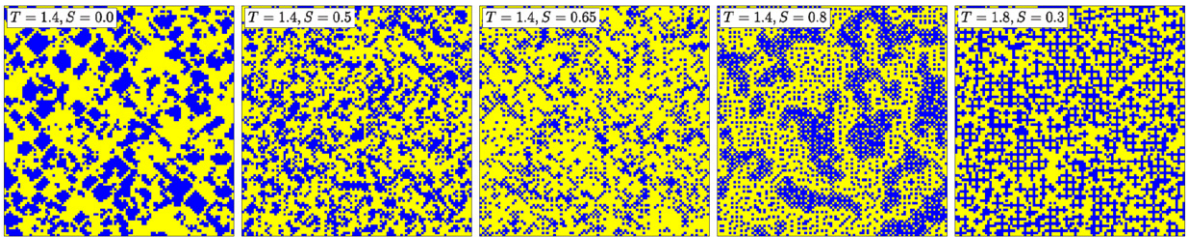

Fig. 4. Snapshots after 10^3 MCS showing typical configurations for several values of T and S for $\rho = 1$. Blue/yellow (black/gray) sites represent cooperators/defectors, respectively. Larger levels of cooperation are associated with the presence of a long tail in the group size distribution, while the compactness of the large cooperator groups depends on S, being large (small) for small (large) S. Notice that the rightmost snapshot is the only one with $T = 1.8$. In this last case, 2×2 squares of defectors separated by lines of cooperators form a fully stable structure since $p(K_1^4) > p(K_0^2) > p(K_1^2)$. Because of the random initial state, we only observe patches of such structure.

For the region around $S = 0.65$, the only difference in the ranking of payoffs is that we now have $p(K_1^1) > p(K_0^2)$, while for $S = 0.5$ it was $p(K_1^1) < p(K_0^2)$. Interestingly, although a cooperator with a single cooperative neighbor fares better for $S = 0.65$ than for 0.5, when compared with a defector with two cooperating neighbors, the density of cooperators is strongly reduced when compared with the neighboring regions.

If one ranks all values of $p(K_\theta^n)$, for the values of T and S considered in Fig. 4, as S increases, the unique modification is that $p(K_0^2)$ moves further down in the payoff ranking. For $S = 0.8$, for example, $p(K_0^2)$ and $p(K_1^0)$ switch places (when compared with $S = 0.65$) and $p(K_0^2) < p(K_1^0)$. A sublattice of cooperators (or, equivalently, defectors) separated by every other site is stable, while the intermediate sites may flip from one to the other. For a random initial state, the lattice will be populated with small patches of such a stable structure. In the PD region, cooperation is sustained by compact groups of cooperators while they decrease in compactness as S becomes larger, accompanied by an increase of cooperator–defector interfaces, since unilateral cooperation becomes worthwhile. It is important to emphasize that although it seems at first that the increase of S would enhance cooperation in a population, what it indeed promotes is a continued interaction between cooperators and defectors, since the punishment for being exploited decreases. In fact, one may introduce a measure of such exploitation as the relative number of CD pairs (ρ_{per}), also related to the total perimeter of cooperator clusters and shown in Fig. 3, bottom panel. These interfaces can also be directly observed in the snapshots of Fig. 4, in the form of checkerboard-like regions in which large groups of cooperators exist with nested defectors. Notice that although ρ_c is not monotonic in S, ρ_{per} is an almost monotonically increasing function of S (the region $0.6 < \rho < 0.7$ is very particular: besides the strong depression in the amount of cooperators, it also breaks the monotonicity, as a function of S, of both ρ_{per} and the fraction of strategy switching, i.e. active, sites, ρ_a).

Interestingly, the elongated structures of cooperators in the SD game, observed in the rightmost snapshot of Fig. 4, are similar to those observed in Ref. [47] although the dynamics and the parameters are not the same, indicating that the results found here for a specific dynamical rule may be more generally valid. In addition, those dendritic structures are but one way of creating large interface structures, alternatives being isolated cooperators or checkerboard-like groups [48].

2.2. *Diluted lattices* ($\rho < 1$) *without mobility* ($m = 0$)

Disorder may be included in these games in several different ways, for example, as site [6] or bond [49] dilution. We consider here the former, once the mobility mechanism that we will later use is dependent on the existence of empty sites. In Ref. [6] we have seen that, for the weak version of the PD game, a small amount of disorder gives rise to pinning points that prevent the strategy switching waves from traversing the system. Indeed, groups of cooperators can be shielded by empty sites, what could be interpreted as natural landscape defenses, and keep their strategy for long intervals of time. These long lasting strategies may be observed, for example, by measuring the persistence function, the fraction of agents that did not switch strategy since $t = 0$. The existence of an asymptotic zero persistence has been shown [6] to be related to the existence of an expressive number of active sites (those that changed strategy since the last time step) at larger densities, while for smaller ones the persistence attains a finite plateau and there is a vanishing number of such active sites. In particular, there is an optimal intermediate density at which cooperators have a maximum population, what remains valid even when the imitating updating dynamics is stochastic [7]. In this last case, in which the optimal cooperative state is closely related to the percolation threshold [7], the existence of fractal clusters at the threshold seems to be important as neither disconnected nor compact clusters are present that help defectors to invade and exploit cooperator communities.

We here extend the results of Ref. [6] for other values of S (see also Ref. [17]), and explore its microscopic interpretation. The introduction of empty sites changes the phase diagram by allowing new configurations of local structures. Therefore, the phase diagram will be composed by the lines that were already present in the case without empty sites, Fig. 2, plus a few more. Besides such new phases, the amount of cooperation will also depend on the total density ρ [6].

Extending the notation introduced earlier, the local neighborhoods shall be denoted by K_θ^{ne}, where $\theta \in \{0, 1\}$ describes the occupation of the center cell, $e \in \{0, 1, 2, 3, 4\}$ gives the total number of empty sites in the local neighborhood and $n \in \{0, 1, 2, 3, 4\}$ ($n \leq 4 - e$ and $n_0 \neq 0$) gives the total number of cooperators in the local neighborhood. Now, the number

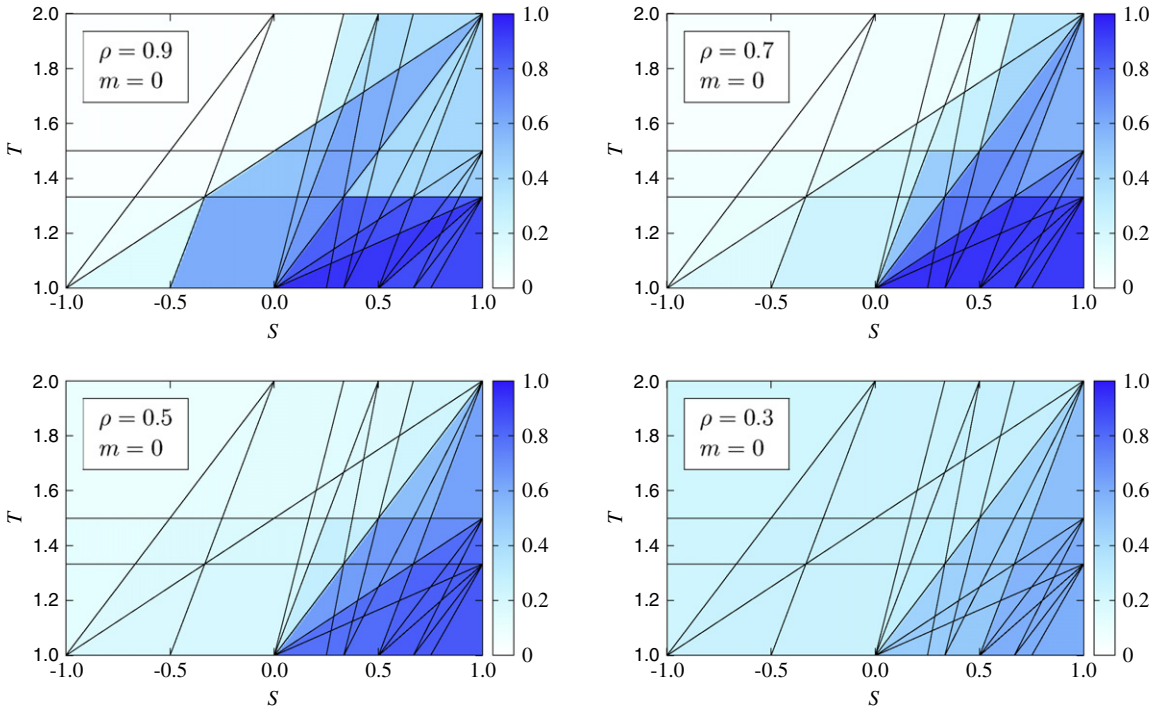

Fig. 5. Phase diagram for diluted lattices without mobility ($m = 0$) and several densities ρ. The color code indicates the level of cooperation ρ_c/ρ. The solid lines represent the functions $f_{n_0n_1e_0e_1}$ which delimit different phases. Although the levels of cooperation are quite similar to those of Fig. 2, a few more lines (and, consequently, a large number of new phases) are introduced due to dilution. This is the case of the four lines that cross at $(S, T) = (1, 3/2)$ and another one that passes through the point $(1, 3)$. In the bottom figures, for $\rho = 0.3$ and 0.5, cooperation is sustained, even if at low levels, in all regions.

of defectors is given by $4 - n - e$. In this way, we have $K_\theta^{n0} \equiv K_\theta^n$. In addition to the functions given in Eq. (1), the following functions which compare the local neighborhoods $K_0^{n_0e_0}$ and $K_1^{n_1e_1}$, with $e_1 \neq 0$, should also be taken into account

$$f_{n_0n_1e_0e_1} = \frac{n_1R + [4 - (n_1 + e_1)]S - [4 - (n_0 + e_0)]P}{n_0}. \tag{2}$$

Using the above notation, $f_{n_0n_100} \equiv f_{n_0n_1}$. Not all of these functions are used, since many give conditions in the region $T \leq R$ (valid for other games).

The values of (n_0, n_1, e_0, e_1) that contribute to the diagram in the range $T > R$ and which lead to functions different from the ones listed for the case $\rho = 1$ are: (2, 3, 0, 1), (2, 2, 0, 1), (2, 1, 0, 1), (2, 0, 0, 1), (1, 3, 0, 1), (1, 2, 0, 1), (1, 1, 0, 1), (1, 0, 0, 1), (1, 0, 0, 2), (1, 2, 0, 2) ≡ (2, 4, 0, 0) and (1, 1, 0, 2) ≡ (2, 2, 0, 0). It should be noted that this diagram is only valid for the case $P = 0$, because in this case a D with a D neighbor is equivalent to a D with an empty neighbor. If $P \neq 0$, then these two configurations are not the same, what will give rise to further phase separating lines. Fig. 5 shows the diagrams for several values of ρ. For $\rho = 0.9$, it is not very different from the full $\rho = 1$ case, apart from an intensification of cooperation in the lower right corner of the figure, what is consistent with the results of Refs. [6,7] that showed that a small amount of quenched dilution is an enhancement factor for cooperation as it prevents defectors from invading cooperator clusters. Stronger deviations are observed for $\rho = 0.5$: although presenting cooperation in the whole region shown, the phases that presented cooperation previously now have a smaller density of cooperators. For small densities, mainly below the percolation threshold, the fate of isolated clusters only depends on their initial composition of Cs and Ds. Thus, regions that were previously unable to sustain cooperation now have small but finite fractions of cooperators (e.g., in the left top corner of the phase diagrams in Fig. 5). For even smaller densities, the final configuration differs little from the initial one, ρ_c tends to 1/2 and the phase diagram becomes homogeneous, independent of S and T.

An example of the sudden transitions occurring at the delimiting lines between phases is shown in Fig. 6 for a cut at $T = 1.4$ for several densities [17]. Again, the transitions can be observed as jumps in the value of ρ_c at the specified points. The most notable transition occurs at $S = 0.4$: depending on the total density ρ, the fraction of cooperators may either jump upwards or downwards, and the change is much more pronounced than for $\rho = 1$. Cooperation is enhanced at intermediate densities and may even fare better than the mean field (e.g., for $\rho = 0.5$ and 0.7 in the figure). The structures formed by cooperators also follow the overall pattern observed for $\rho = 1$ and a few examples are shown in Fig. 8: compact groups in the PD game (left column) and dendritic or checkerboard like in the SD game. For $S = 0$ (left column), although the ever present small cooperator clusters start to increase in size after the percolation threshold, only well above this transition

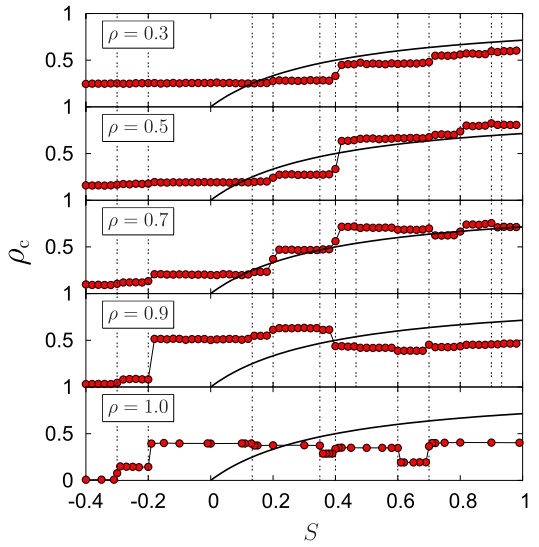

Fig. 6. Average fraction of cooperating individuals ρ_c versus S ($T = 1.4$, $R = 1$ and $P = 0$) for different values of the density ρ without mobility ($m = 0$). The panel at the bottom shows, as vertical lines, the transition points for $\rho = 1$: $S = -0.3$, -0.2, $2/15$, 0.35, 0.4, 0.6 and 0.7. In the remaining panels, in which $\rho < 1$, new transitions appear at $S = 0.2$, $7/15$, 0.8, 0.9 and $14/15$. Interestingly, besides the transition at $S = 0.4$ representing a strong change in ρ_c, whether the jump is upward or downward depends on the value of ρ. Also shown (curved line) is the mean field result. Notice that for large values of S, small and large densities fare worse than the mean field and cooperators perform better only for intermediate densities in the presence of spatial correlations.

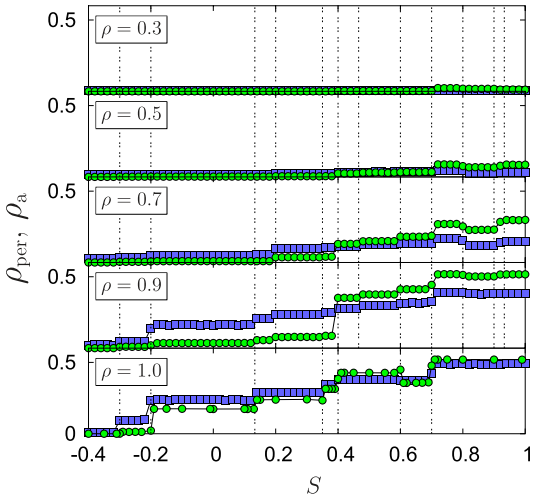

Fig. 7. Average fraction ρ_a of active (green/light gray circles) and pairs of opposite strategies (blue/dark gray squares), ρ_{per}, versus S ($T = 1.4$, $R = 1$ and $P = 0$) for different values of the density ρ without mobility ($m = 0$). The transition lines follow Fig. 6.

point do they occupy a large fraction of the network. The optimal density for cooperators is not that high when stochastic rules are used, being shifted towards the threshold [7]. For $S = 0.8$ (right column), on the other hand, cooperators group themselves into dendritic or checkerboard structures (or stay isolated).

The density of cooperators is monotonic in S only for very low densities, Fig. 6, while for large S (most notably for $S > 0.4$), ρ_c tends to decrease and becomes non monotonic. More information can be obtained by measuring the fraction of active sites, ρ_a, and the fraction of pairs of different strategies, ρ_{per}, as shown in Fig. 7. For low densities, $\rho = 0.3$ and 0.5 in Fig. 7, the configuration is almost frozen and both quantities are very close to zero. Otherwise, they present a tendency to increase with S (albeit exceptional intervals are still present). Interestingly, although there seems to be a correlation between the two parameters for all densities, deviations are stronger close to the optimum density (see the case of $\rho = 0.9$ in Fig. 7).

2.3. *Diluted lattices* ($\rho < 1$) *with mobility* ($m \neq 0$)

In the case $m = 0$ studied in Ref. [6] ($T = 1.4$ and $S = 0$), and for the noiseless imitation rule considered here, the fraction of cooperators starts to increase again around the site random percolation threshold ($\rho \simeq 0.593$ in the square

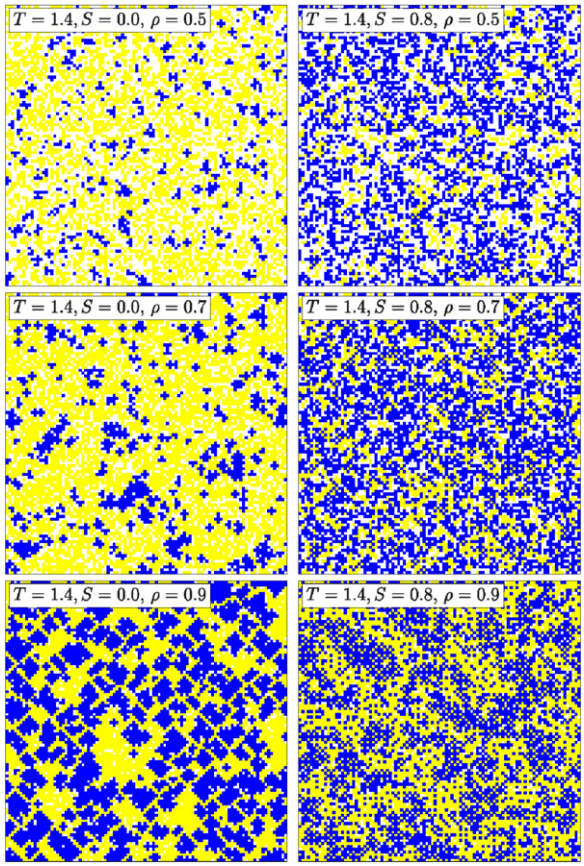

Fig. 8. Snapshots for $m = 0$, after 10^4 MCS, showing typical configurations for several values of S with $T = 1.4$ and densities both below and above the site random percolation threshold ($\rho \simeq 0.59$). Blue/yellow (black/gray) sites represent cooperators/defectors, as in Fig. 4, while white ones are empty sites. Notice that for a given density, the empty sites in these snapshots are in the same position.

lattice). At low densities, cooperators persist on some isolated clusters because of a favorable initial condition that allowed them to overcome defectors. In this regime, and depending on how mobility is implemented, defectors may act as free riders that eventually exploit the whole system (remember that random diffusion is a disaggregating factor), leading to the extinction of cooperators. As shown in Ref. [13], there is a minimum density above which cooperators are able to survive in the presence of mobility. Although in some cases such density is above the percolation threshold, and cooperation seems to need an underlying percolating cluster in order to be maintained when $m \neq 0$, cooperation may also resist below the percolation threshold. Indeed, with a smaller temptation, isolated groups of cooperators are less predated by defectors and are able to survive.

Whether or not the phase diagram changes when random mobility is also taken into account depends on the details of the diffusion. When the offspring step is performed before the diffusion (COD—combat–offspring–diffusion dynamics—in the notation of Ref. [13]), no new transition appears, and the phase diagram has the same cross sections as those of the previous section, whatever the value of m, albeit with different fractions of ρ_c in each phase. These diagrams are shown in Fig. 9. Notice that many regions now are fully dominated by defectors. In general, low mobility (left column) is more favorable to cooperation: besides being present in more regions of the phase diagram, the fraction of cooperators is also higher. However, the SD game benefits much more from mobility than the PD, as most of the shaded regions are located for $S > 0$. The latter, in particular, only presents a finite fraction of cooperators for high densities (see also Ref. [17]). Although it is difficult to summarize its general behavior, the SD game fares better at intermediate densities. In the snapshots of Fig. 10 we observe how cooperators are able to build clusters even in the presence of random mobility. These clusters, however, are less compact than those for the case without mobility, Fig. 8. An interesting aspect in those snapshots is the presence of defector and cooperator-free regions. In the upper row, for $\rho = 0.7$ (above the percolation threshold), cooperators aggregate in isolated domains while the defectors percolate throughout the lattice. In the bottom row, on the other hand, although the connected domains are smaller, a different kind of order can be observed: cooperators and vacant sites form large regions free of defectors. These cooperators, due to the rattling aspect of diffusion, are indeed correlated. Moreover, these defector-free regions now percolate. For this COD dynamics, the agents do not carry any payoff with them, since the combat and offspring steps are performed in succession before diffusion. In other words, there is no memory of the previous location.

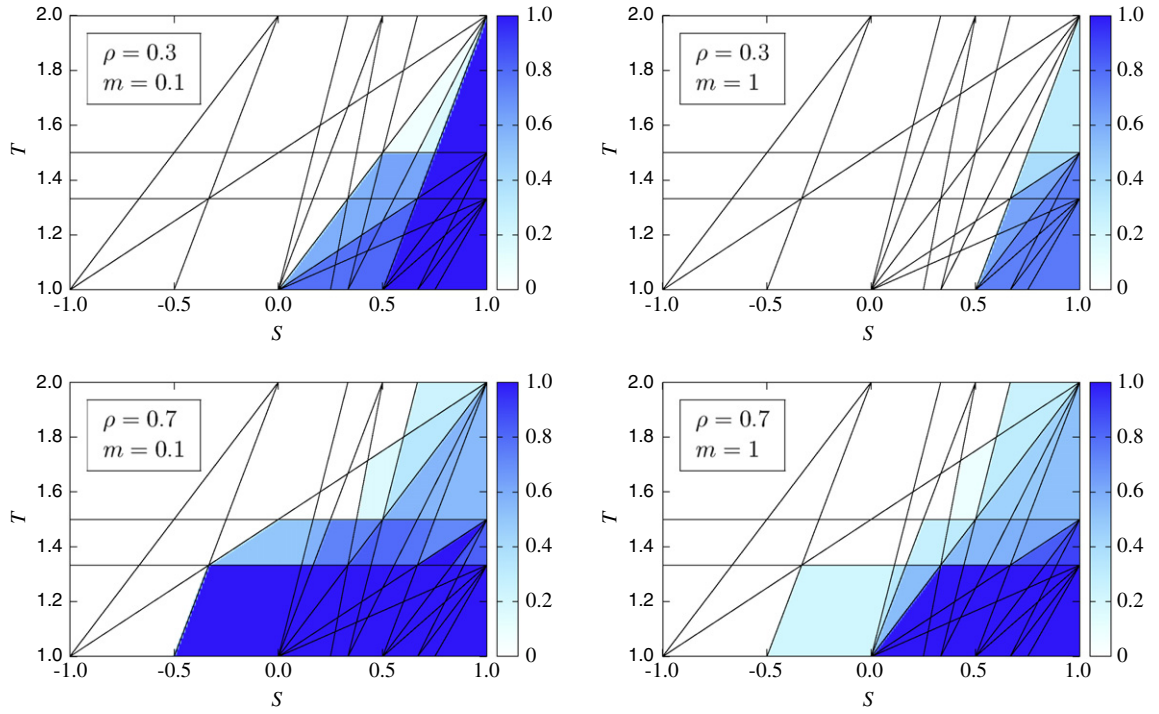

Fig. 9. Phase diagrams for the case in which the diffusive step is taken after the offspring generation (COD). The smaller mobility has more cooperative regions in the phase diagram (blue) and an overall higher level of cooperation in each region. Notice also that the PD game does not present cooperation at low densities. (For interpretation of the references to color in this figure legend, the reader is referred to the web version of this article.)

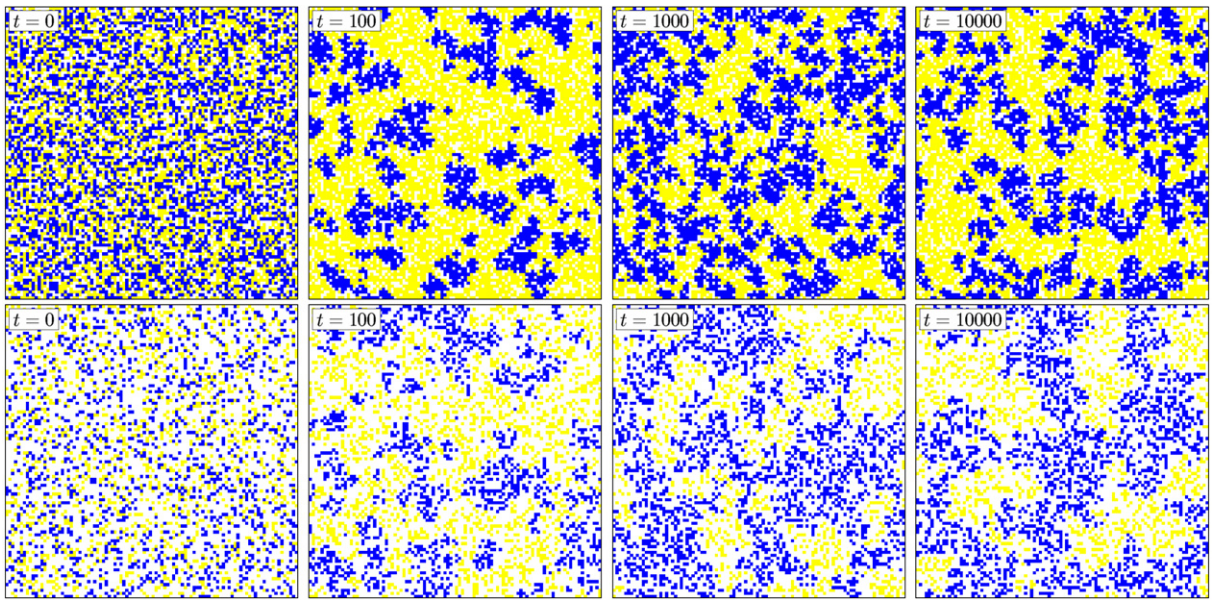

Fig. 10. Snapshots for $m = 0.1$ and $T = 1.4$ with COD dynamics for several times, showing typical configurations. The top row is for $\rho = 0.7$ and $S = 0$, while the bottom row shows $\rho = 0.3$ and $S = 0.5$. Blue/yellow (black/gray) sites represent cooperators/defectors, as in Fig. 4, while white ones are empty sites. The bottom row, despite its small density (below the percolation threshold), has percolating defector-free regions. The upper row presents, on the other hand, cooperator-free percolating regions.

Although evaporation is an important mechanism to decrease cooperation (cooperators that move away from the surface of clusters tend to become defectors), when its rate is not too large or if diffusion is prevented by geometric hindrance at larger densities, clusters may be stable. If the cluster surface is locally flat, cooperators located at the surface make contact with three other cooperators and have high payoff. Moreover, they also compare their payoff with interior cooperators

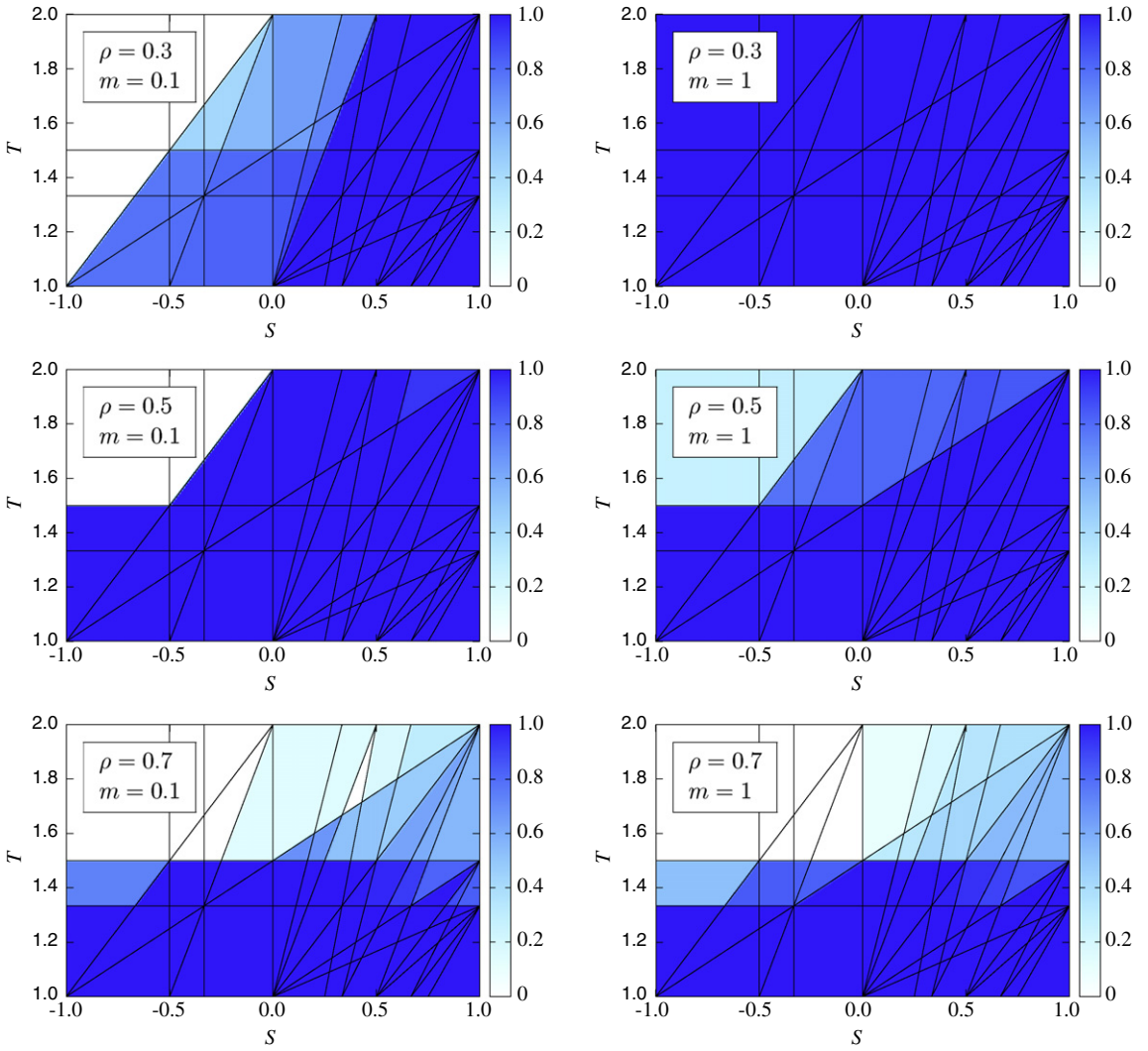

Fig. 11. Two dimensional cross section of the phase diagram when mobility is considered after the combats (CDO dynamics). Notice that although for $m = 1$ the density of cooperators is monotonic, for $m = 0.1$ it is not, and intermediate densities sustain more cooperation.

whose payoff is even larger. These regions are prone to cooperation and any defector that, after diffusion, gets in contact with the cooperative surface will be assimilated. This is the basic growth mechanism in the COD case.

The phase diagram for the CDO (combat–diffusion–offspring) case is slightly different from the one for empty sites or COD dynamics. This is due to the fact that in them, the configurations given by $K_0^{0e_0}$ (D without cooperating neighbors) never compete with any $K_1^{n_1e_1}$ (C with cooperating neighbors) configuration. In the CDO, however, since the diffusion step occurs between the contest and the generation of offspring, the confrontations described above are possible due to the change in configuration between the two steps. Therefore, by taking these new possibilities into account, a few more lines should contribute to the phase diagram, namely

$$g_{(n_0=0,n_1,e_0,e_1)} = \frac{(4-e_0)P - n_1R}{4-(n_1+e_1)}, \tag{3}$$

which are valid for $n_0 = 0$ and $n_1 + e_1 \neq 4$. If the latter inequality is not satisfied, the functions will give rise to conditions on R and P. These functions mark transitions at $S = g_{(n_0=0,n_1,e_0=0,e_1)}$, for the different possible values of n_1, e_1 and e_0. For $R = 1$ and $P = 0$, this means that there will be new transition points at the following values of S: -3, -2, -1, $-1/2$, $-1/3$ and 0, independent of e_0. No new transition appears for $S > 0$. It is interesting to notice that due to the new transition line at $S = 0$, this is the only case (besides the mean field) in which the regions around the weak PD case ($S = 0$) differ. These lines are shown in Fig. 11 for several values of ρ and m. Most of the regions are fully dominated by cooperators, although a few regions (mainly at small S, large T) are cooperator free. As shown in Fig. 11, right column, the high mobility case ($m = 1$) is more favorable to cooperation at low densities. On the other hand, for low mobilities (left column), at

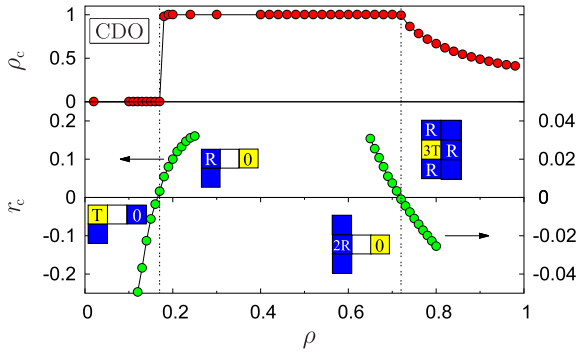

Fig. 12. Top: average fraction of cooperating individuals for CDO dynamics, $m = 1$, $T = 1.4$ and $S = 0$. For intermediate densities, cooperators dominate. At low densities ($\rho \lesssim 0.18$) there is a discontinuous transition to a phase in which all agents become defectors while at high densities, $\rho \gtrsim 0.73$, the all C state continuously turns into a mixed strategy phase. Bottom: order parameters indicating the leading microscopic processes originating the intermediate all C phase. We also indicate the more relevant microscopic process in each region. Yellow/light gray are defectors, blue/dark gray are cooperators, and white boxes are empty sites to which one of the agents may jump. The letters indicate the payoff accumulated by the combating agents. Notice that the rightmost process is not diffusive. Below $\rho \simeq 0.18$, since it has a C neighbor, the defector has payoff T when it collides with the single cooperator whose payoff is zero, winning the combat. On the other hand, above $\rho \simeq 0.18$, the cooperator with payoff R, because of its C neighbor, outperforms the defector whose payoff is zero. Being the dominant process, this leads to a fast increase in the population of cooperators. Up to $\rho \simeq 0.73$, cooperators still have an advantage when interacting with defectors after the jump, since they had accumulated enough payoff from their previous interaction. However, above this value of ρ, a non diffusive process, reminiscent of the original, full density PD game, allows defectors to invade previously cooperative regions, thus decreasing ρ_c.

intermediate densities the fraction of cooperators is larger. Differently from the COD dynamics, here the agents move after the combat and thus carry part of their previous history along. This memory of their recent combat is important to understand the mechanism responsible for the enhancement of cooperation. As an illustration, consider the case studied in Ref. [13] in which a C dominated phase occurs for $0.18 \lesssim \rho \lesssim 0.73$ for $T = 1.4$, $S = 0$ and $m = 1$ (top row of Fig. 12). For the low densities close to $\rho \approx 0.18$ the mechanism does not rely on the existence of a spanning cluster of agents. Indeed, the largest occurrence is of single and two agent clusters. The transition rate r_c with which defectors become cooperators depends on the local neighborhood of the two agents at the moment in which their payoffs were collected (combat) and has two main contributions: $r_c = \mathrm{Prob}(K_1^{1e_1}, K_0^{0e_0}) - \mathrm{Prob}(K_1^{0e_1}, K_0^{1e_0})$, where the probabilities are the number of the given encounter divided by the total number of active sites averaged over time in the beginning of the simulation ($t \leq 100$). That is, the number of cooperators increases when a C with one C neighbor ($K_1^{1e_1}$) meets, after the jump, a D without C neighbors ($K_0^{0e_0}$) and decreases when a D also with one C neighbor ($K_0^{1e_0}$) meets, after the jump, a C without other C neighbors ($K_1^{0e_1}$). In the bottom row, left side, of Fig. 12 we depict these processes, each one in the region in which it is dominant, along with the curve showing that r_c changes sign around the point at which the density of cooperators explodes. What changes from one case to the other as ρ increases is that clusters with an increasing number of agents become more common and give support to the stability of the CC pair.

This transition at low densities does not occur in the COD dynamics and is the mechanism that allows a C to leave a C cluster and continue cooperating in the CDO dynamics.

The region in which the fraction of cooperators starts to decrease ($\rho \gtrsim 0.73$) is above the percolation threshold, the system is denser and it is much more likely that an individual has several neighbors. Consequently, the microscopic process responsible for this decrease is different from the previous one. In effect, the observed decrease in the density of cooperators as the lattice approaches full occupancy is rather general, non diffusive and reminiscent of the $m = 0$ behavior for increasing densities [6]. Indeed, as the number of empty sites decreases, irrespective of the mobility, the number of active sites increases, signaling that there is less defect-induced pinning in the system and cooperators become more vulnerable to defectors. The mobility m, also being a depinning mechanism, plays a role by shifting the transition to smaller values of ρ. It should be noted that the main microscopic processes that drive a given transition are dependent on the values of T and S, besides the system occupancy, because a change in ρ modifies the expected number of neighbors that each individual has. In the particular case of Fig. 12, we may also point that, differently from the low density transition, there are many microscopic processes that are relevant for increase of defectors. As an example, consider those associated with neighborhoods $K_1^{2e_1}$ and $K_0^{0e_0}$ (D $\to$ C) or $K_1^{1e_1}$ and $K_0^{3e_0}$ (C $\to$ D). We show in the right part of Fig. 12, the order parameter that can be built from these processes, $r_c = \mathrm{Prob}(K_1^{2e_1}, K_0^{0e_0}) - \mathrm{Prob}(K_1^{1e_1}, K_0^{3e_0})$, and how it changes sign at the transition. There are, however, other possible combinations of microscopic processes giving rise to order parameters changing sign in this region (although not necessarily at the same precise value).

For the COD dynamics, it is also not easy to single out a few processes that are responsible for changing the amount of cooperators.

As an example, we consider the case $T = 1.4, S = 0$ and very low mobility ($m = 0.01$) studied in Ref. [13]. The larger the mobility, the larger is the density capable of supporting cooperation. For $m \to 0$, this minimum density seems

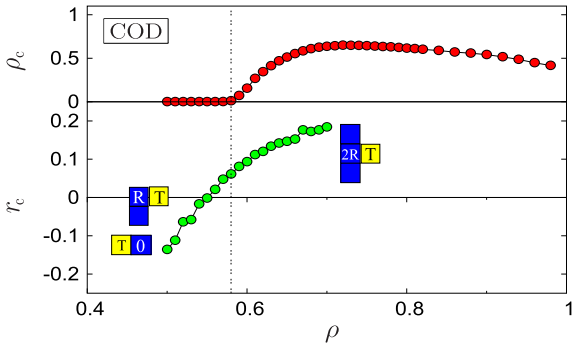

Fig. 13. Top: average fraction of cooperating individuals for the COD dynamics, $m = 0.01$, $T = 1.4$ and $S = 0$. The system presents a transition from a cooperator-free phase to a coexistence phase near the percolation threshold $\rho \simeq 0.59$ for the square lattice. Below this density, the evaporation of C clusters is not counterbalanced by any mechanism and diffusion is detrimental to the population. Bottom: order parameter associated with the leading microscopic processes that localize the transition to the coexistence state. Notice that the processes depicted here are only a few of those existing at this density (also explaining why the curve does not cross at the right value).

to approach the random site percolation threshold. Above the transition, in the phase presenting both cooperators and defectors, there is a great chance that an individual has 2 or 3 neighbors. The main microscopic mechanisms responsible for the transition are three encounters: $K_1^{2e_1}$ and $K_0^{1e_0}$ (D $\rightarrow$ C); $K_1^{1e_1}$ and $K_0^{2e_0}$ (C $\rightarrow$ D); $K_1^{0e_1}$ and $K_0^{1e_0}$ (C $\rightarrow$ D). The latter corresponds to a C player leaving a C cluster and meeting a D. In Fig. 13, we show the order parameter $r_c = \text{Prob}(K_1^{2e_1}, K_0^{1e_0}) - \text{Prob}(K_1^{1e_1}, K_0^{2e_0}) - \text{Prob}(K_1^{0e_1}, K_0^{1e_0})$, where the probabilities are calculated as above in the CDO case.

It takes the value 0 at $\rho \simeq 0.56$, slightly below the transition density. This small difference is due to the fact that many other, less frequent processes have not been included in the order parameter. It should be noted that as the mobility probability m increases, the evaporation of C clusters becomes greater and the transition is driven to higher values of ρ. At these higher concentrations, many other microscopic processes become important to determine the value of ρ at which the transition occurs.

3. Conclusions

We presented a systematic study of the Prisoner's Dilemma and Snowdrift games, with and without random mobility, when the evolution follows a non stochastic imitation rule in which all agents, in parallel, choose to follow their more successful neighbor. Few attempts have been made in the literature [4,39,41,43,44,46] to present a comprehensive account of the possible behaviors of such evolutionary games. Due to the large number of parameters and possible dynamical rules in such models, comparisons among them are difficult and the universality of the results difficult to access. The phase diagrams and the corresponding transition lines are obtained by enumerating all possible local configurations, while the fraction of cooperators in each phase is measured in Monte Carlo simulations. Some of the regions appearing in these phase diagrams may also be obtained [46] from the analysis of the fundamental clusters growth conditions. However, when disorder is present (for example, as dilution), there are finite size sample to sample fluctuations that depend on the random initial conditions and the disorder realization. In this case, the cooperative fate of the population must be obtained through an average over the disorder and initial states. Although here we only considered the stationary, asymptotic properties of the model, it is interesting to notice that the different regions of the phase diagram may have their dynamic properties characterized by a Lyapunov exponent [46], the active region where Cs and Ds coexist being mostly chaotic (positive Lyapunov exponents).

Mobility, in its random flavor considered here, is a stochastic element that not only prevents the system from being trapped in a frozen state but may also strongly enhance the amount of cooperation in the system, despite its tendency to evaporate and disaggregate clusters. Besides exploring, in the universe of parameters of a particular version of these games, the conditions under which cooperation may be amplified by spatial and mobility factors, we also discussed the microscopic mechanisms responsible for such behavior. Whether a backbone of supporting agents is essential, actually depends on the dynamics and the parameters involved. In fact, the parallel noiseless dynamics considered here tends to mask the role of the percolating cluster [7]. An intriguing feature is that instead of smoothing out transitions, when compared with the immobile system, a few extra transitions are indeed driven by mobility. Interestingly, the CDO case presents a new transition separating the semi-planes $S < 0$ (PD) and $S > 0$ (SD). The other situation in which this transition appears is within mean field. Thus, it differs from the other cases considered here in which the so called weak version of the PD game presents the same behavior for both $S = 0^+$ and $S = 0^-$.

Assuming that the timescale for collecting the payoffs (the combat phase) and the interval between generating offspring are of the same order, the order in which these steps are taken becomes relevant. In particular, the growth mechanism of cooperating clusters differs whether the diffusive step is performed after or before the reproduction step. In the former (COD), cooperators have no memory of their previous encounters, carry no payoff while diffusing and may be easily

converted to defectors once they move away from the protective zone of cooperative clusters. However, diffusing defectors may be assimilated by these clusters and this passive mechanism may increase cooperation when mobility is not extremely high or density is not too low. In the latter case (CDO), on the other hand, the agents have memory of their previous location and may carry a large payoff, thus enabling cooperators to actively invade regions away from the percolating cluster. The amount of cooperation in this case is much larger than in the previous one.

In diffusive games, there are two competing parameters: density and diffusivity. While larger densities increase the correlation between neighbors, the effect of random diffusion depends on the density and sometimes decreases correlation. It would then be important to compare the results presented here with those using different updating and diffusion (random) rules, for example, by allowing multioccupation and position swapping [15,16] or different timescales of the selection and fitness collection processes [20].

A caveat that must be emphasized concerns the phase diagrams and the fraction of cooperators measured in the simulations. Although the transition lines are exact, the densities of cooperators depicted in the previous phase diagrams may slightly change when larger system sizes and longer simulation runs are used. Finite size effects are usually not taken into account once actual populations are finite both in time and space, but are of interest for a better understanding of the model.

In summary, we presented a comprehensive study of the PD and SD games under a deterministic synchronous updating rule in the presence of quenched and annealed defects. The different phases in the *TS* plane and the effects of dilution and mobility were discussed along with the corresponding microscopic mechanisms. Under a wide range of conditions, we have shown that mobility, even if random, may be responsible for a dramatic increase in the population of cooperators.

Acknowledgments

The research was partially supported by the Brazilian agencies CNPq, grant PROSUL-490440/2007, CAPES and Fapergs. We thank Hugo Fort and Ana T.C. Silva for collaborating in subjects related to this project. JJA thanks the INCT-Sistemas Complexos (CNPq) for support and the LPTHE (UPMC, Paris) where part of this paper was written during his stay.

References

[1] M. Doebeli, C. Hauert, Ecol. Lett. 8 (2005) 748.
[2] M.A. Nowak, Science 314 (2006) 1560.
[3] G. Szabó, G. Fáth, Phys. Rep. 446 (2007) 97.
[4] C.P. Roca, J.A. Cuesta, A. Sánchez, Phys. Life Rev. 6 (2009) 208.
[5] M. Perc, A. Szolnoki, BioSystems 99 (2010) 109.
[6] M.H. Vainstein, J.J. Arenzon, Phys. Rev. E 64 (2001) 051905.
[7] Z. Wang, A. Szolnoki, M. Perc, Nature Sci. Rep. 2 (2012) 369.
[8] L.A. Dugatkin, D.S. Wilson, Amer. Nat. 138 (1991) 687.
[9] M. Enquist, O. Leimar, Anim. Behav. 45 (1993) 747.
[10] R. Ferrière, R.E. Michod, Amer. Nat. 147 (1996) 692.
[11] I.M. Hamilton, M. Taborsky, Proc. R. Soc. B 272 (2005) 2259.
[12] J.-F. Le Galliard, F. Ferrière, U. Dieckmann, Amer. Nat. 165 (2005) 206.
[13] M.H. Vainstein, A.T.C. Silva, J.J. Arenzon, J. Theoret. Biol. 244 (2007) 722.
[14] G. Jian-Yue, W. Zhi-Xi, W. Ying-Hai, Chin. Phys. 16 (2007) 3566.
[15] S. Számadó, F. Szalai, I. Scheuring, J. Theoret. Biol. 253 (2008) 221.
[16] M. Droz, J. Szwabiński, G. Szabó, Eur. Phys. J. B 71 (2009) 579.
[17] E.A. Sicardi, H. Fort, M.H. Vainstein, J.J. Arenzon, J. Theoret. Biol. 256 (2009) 240.
[18] H. Yang, B. Wang, Chin. Sci. Bull. 56 (2011) 3693.
[19] S. Suzuki, H. Kimura, J. Theoret. Biol. 287 (2011) 42.
[20] A. Gelimson, J. Cremer, E. Frey, Phys. Rev. E 87 (2013) 042711.
[21] H. Cheng, H. Li, Q. Dai, Y. Zhu, J. Yang, New J. Phys. 12 (2010) 123014.
[22] H.-X. Yang, Z.-X. Wu, B.-H. Wang, Phys. Rev. E 81 (2010) 065101(R).
[23] H. Cheng, Q. Dai, H. Li, Y. Zhu, M. Zhang, J. Yang, New J. Phys. 13 (2011) 043032.
[24] H. Lin, D.-P. Yang, J. Shuai, Chaos Solitons Fractals 44 (2011) 153.
[25] Y.-T. Lin, H.-X. Yang, Z.-X. Wu, B.-H. Wang, Physica A 390 (2011) 77.
[26] D. Helbing, W. Yu, Proc. Natl. Acad. Sci. 106 (2009) 3680.
[27] D. Helbing, Eur. Phys. J. B 67 (2009) 345.
[28] W. Yu, Phys. Rev. E 83 (2011) 026105.
[29] C.A. Aktipis, J. Theoret. Biol. 231 (2004) 249.
[30] L.-L. Jiang, W.-X. Wang, Y.-C. Lai, B.-H. Wang, Phys. Rev. E 81 (2010) 036108.
[31] C.A. Aktipis, Evol. Hum. Behav. 32 (2011) 263.
[32] Z. Chen, J. Gao, Y. Cai, X. Xu, Physica A 390 (2011) 1615.
[33] J. Zhang, W.-Y. Wang, W.-B. Du, X.-B. Cao, Physica A 390 (2011) 2251.
[34] C. Zhang, J. Zhang, F.J. Weissing, M. Perc, G. Xie, L. Wang, PLoS One 7 (2012) e35183.
[35] S. Meloni, A. Buscarino, L. Fortuna, M. Frasca, J. Gómez-Gardeñes, V. Latora, Y. Moreno, Phys. Rev. E 79 (2009) 067101.
[36] J.C. Koella, Proc. R. Soc. B 267 (2000) 1979.
[37] A. Rapoport, Two-Person Game Theory, U. of Michigan, Ann Harbor, 1966.
[38] M.A. Nowak, R.M. May, Nature 359 (1992) 826.
[39] C.P. Roca, J.A. Cuesta, A. Sánchez, Phys. Rev. E 80 (2009) 046106.
[40] M.A. Nowak, R.M. May, Int. J. Bifurcation Chaos 3 (1993) 35.
[41] F. Schweitzer, L. Behera, H. Muhlenbein, Adv. Comput. Syst. 5 (2002) 269.
[42] C. Hauert, Int. J. Bifurcation Chaos 12 (2002) 1531.
[43] F.C. Santos, J.M. Pacheco, T. Lenaerts, Proc. Natl. Acad. Sci. 103 (2006) 3490.
[44] M. Tomassini, L. Luthi, M. Giacobini, Phys. Rev. E 73 (2006) 016132.
[45] P.-P. Li, J. Ke, Z. Lin, P.M. Hui, Phys. Rev. E 85 (2012) 021111.
[46] C. Hauert, Proc. R. Soc. London B 268 (2001) 761.
[47] C. Hauert, M. Doebeli, Nature 428 (2004) 643.
[48] G. Szabó, A. Szolnoki, M. Varga, L. Hanusovszky, Phys. Rev. E 82 (2010) 026110.
[49] M. Lin, N. Li, L. Tian, D.-N. Shi, Physica A 389 (2010) 1753.